Fourier Transform Infrared Analysis of Bacteriorhodopsin Secondary Structure†

Josep Cladera, Manuel Sabés, and Esteve Padrós*

Unitat de Biofísica, Departament de Bioquímica i de Biologia Molecular, Facultat de Medicina, Universitat Autònoma de Barcelona, 08193 Bellaterra, Barcelona, Spain

Received March 30, 1992; Revised Manuscript Received July 7, 1992

ABSTRACT: Fourier transform infrared spectroscopy at a resolution of 1 cm^{-1} has been used to study the conformation of dark-adapted bacteriorhodopsin in the native purple membrane, in H_2O and D_2O suspensions. A detailed analysis of the amide I bands was made using derivative and deconvolution techniques. Curve-fitting results of four independent experiments indicate, after estimation of the methodological errors, that native bacteriorhodopsin contains 52–73% α-helices, 13–19% reverse turns, 11–16% β-sheets, and 3–7% unordered segments. Our analysis has enabled the identification of several components corresponding to α-helices, β-sheets, and reverse turns. Besides the α_I- and α_{II}-helices (peaking at 1658 and 1665 cm^{-1}), we propose that two more infrared bands arise from α-helical structures: one at 1650 cm^{-1} from α_I and another one at 1642 cm^{-1} in H_2O suspension, which could originate from type III β-turns (i.e., one turn of 3_{10}-helix). The relatively high content of reverse turns suggests the presence of one reverse turn per loop, plus another one in the C-terminal segment. On the other hand, several reasons argue that the calculated mean β-sheet content of around 14% should be decreased somewhat. These β-sheets could be located in the noncytoplasmatic links of the bacteriorhodopsin molecule.

The molecular mechanism by which the purple membrane from *Halobacterium halobium* pumps protons under the influence of light has been the subject of extensive investigation in recent years (Stoeckenius & Bogomolni, 1982; Dencher, 1983; Khorana, 1988; Oesterhelt & Tittor, 1989; Henderson et al., 1990). One fundamental aspect of the transport mechanism corresponds to the structural changes of bacteriorhodopsin (BR)[1] that occur during the photocycle (Fodor et al., 1988). Some amino acid residues which participate in these changes have already been identified (Khorana, 1988; Braiman et al., 1988; Lin et al., 1991). It is also important to determine the structural alterations of BR as a consequence of a number of membrane modifications such as delipidation or deionization, which alter the photocycle and the proton-pumping activity to different degrees. Recent low-temperature electron microscopy diffraction studies clearly show the presence of seven α-helices spanning the membrane, at a near-atomic resolution (Henderson et al., 1990). However, there is still insufficient information regarding the conformation of the two ends of the molecule, or the links between the helices.

Fourier transform infrared spectroscopy is one of the most powerful techniques to obtain information about the secondary structure of proteins, owing to the specific hydrogen bonding of the C=O and N–H groups for each kind of structure. However, the conformation-sensitive bands overlap, and thus several techniques have been developed in order to obtain quantitative estimations of the secondary structural classes (Byler & Susi, 1986; Surewicz & Mantch, 1988; Dong et al., 1990; Dousseau & Pézolet, 1990; Lee et al., 1990, 1991). Although none of these methods is devoid of drawbacks, a comparison in terms of the correspondence between the predicted and the known structures reveals that curve-fitting of the deconvoluted spectrum still remains the most reliable method. Indeed, the application of one of the latest proposed methods to BR gives rise to a negative value for the estimation of reverse turns [–11.2%; see Lee et al. (1991)]. On the other hand, the assignment of bands to different types of secondary structure is still subject to certain ambiguity due to partial overlapping of bands corresponding to different secondary structural classes. Thus, the BR model (Henderson et al., 1990) can serve as a guide to interpret the spectroscopic data [see also Glaeser et al. (1991)].

In order to decompose the complex amide I bands into their components, deconvolution and derivative techniques have already been applied to a number of polypeptides and water-soluble and membrane proteins (Byler & Susi, 1986; Surewicz & Mantch, 1988; Dong et al., 1990). The bacteriorhodopsin structure has also been studied using these band-narrowing methods, which have provided evidence for α-helical and other structures (Lee et al. 1987; Duñach et al., 1989; Earnest et al., 1990). Our work is aimed not only to obtain a quantification as accurate as possible of each type of BR secondary structure but also to set up a method and a reference for future comparisons between native and modified BR forms. Our spectra, recorded at a resolution of 1 cm^{-1} with a data-encoding interval of 0.25 cm^{-1}, allow the detection of several types of α-helix, reverse turns, and β-structures. While the absolute quantification is still subjected to several sources of errors, we consider that our results will provide a more accurate means to compare different BR structures. This should allow the detection of subtle conformational changes of BR.

MATERIALS AND METHODS

Sample Preparation. Purple membrane was isolated from *Halobacterium halobium* strain S9 as described (Oesterhelt & Stoeckenius, 1974). Membrane suspensions in water (pH 6.0) at about 20 mg/mL protein concentration were placed in 6-μm path-length CaF_2 IR cells with tin spacers. Suspensions in D_2O were prepared by washing the membrane 3 times with D_2O and keeping the final suspension overnight before data collection, to achieve a good H/D exchange.

† This work was supported by Grant PB89-0301 from the Dirección General de Investigación Científica y Técnica. J.C. acknowledges the award of a fellowship by the DGICYT.

* To whom correspondence should be addressed at Unitat de Biofísica, Facultat de Medicina, Universitat Autònoma de Barcelona, 08193 Bellaterra, Barcelona, Spain. Phone: 3-5811870. Fax: 3-5812004.

[1] Abbreviations: BR, bacteriorhodopsin; IR, infrared; FTIR, Fourier transform infrared; FWHH, full width at half-height.

0006-2960/92/0431-12363$03.00/0

Samples in D_2O (pD 6.0) at a protein concentration of about 20 mg/mL were placed in 25-μm path-length CaF_2 IR cells with Teflon spacers.

Infrared Data Acquisition. IR spectra were acquired on a Mattson Polaris FTIR spectrometer equipped with an MCT detector, working at an instrumental resolution of 1 cm^{-1}. A total of 1000 scans were averaged using a sample shuttle, apodized with a triangle function, and Fourier-transformed. The spectrometer was continuously purged with dry air (dew point lower than −60 °C). The sample temperature (20 °C) was set using a homemade cell jacket of circulating water. To obtain the pure spectra of purple membrane, spectra of the solvent were collected under identical conditions, and subtractions were done with the computer. The criteria for a good subtraction was the removal of the water band near 2130 cm^{-1}, and the obtention of a flat line between 1800 and 2000 cm^{-1}. This same region is also a useful zone to check the absence of residual water vapor peaks. On the other hand, the subtraction of the liquid water contribution proved to be reliable only using the MCT detector.[2] Indeed, the subtractions had to be made very carefully, using the same cell and the same temperature to obtain the appropriate water reference spectra. These constrains were not so severe with the D_2O samples, due to the lack of strongly absorbing bands in the amide I region.

Resolution Enhancement and Curve-Fitting. At the present time, there is some debate about the quantification of the secondary protein structure using curve-fitting methods over deconvoluted IR spectra. The reason is that Fourier self-deconvolution does not affect the original integrated band area provided that the deconvolution function and the original band have the same bandwidth (Mantsch et al., 1988). However, in general the different bands also have different bandwidth values, so it seems likely that some distortions are introduced by the deconvolution procedure. On the other hand, fitting the original, undeconvoluted spectrum usually gives rise to different sets of solutions (due to the lack of definition of the spectrum), even if using as input bands those derived from the fitting of the deconvoluted spectrum. Thus, we followed the method of fitting the deconvoluted spectra (Byler & Susi, 1986), and at the same time we tried to obtain a quantitative assessment of the errors introduced by the entire procedure (resolution enhancement plus curve-fitting). We constructed synthetic spectra by adding 14 overlapped bands (with bandwidths between 12 and 20 cm^{-1}), which were the result of curve-fitting the deconvoluted experimental spectra, converting the bands to 100% Lorentzian, and multiplying the half-width by 2.5 (the k factor). Thus, the synthetic spectra were almost identical with the original ones. These spectra were Fourier-derivated, self-deconvoluted, and curve-fitted using the programs developed by Moffatt et al. (1986). The results obtained can be summarized as follows.

(*i*) *Fourier Derivation of the Synthetic Spectra.* Using Fourier self-derivative, we detected almost all the component bands. Normally, bands of similar bandwidth, with maxima separated less than 5 cm^{-1}, were not resolved. The increase of the breakpoint[3] from 0.1 to 0.3 did not increase the derivative resolution. When we added to the original synthetic spectrum a similar noise level to that of the experimental spectra and increased the breakpoint, new peaks appeared in the derivative. A safety interval of breakpoint values for the resolution employed (1 cm^{-1}) was found to be between 0.10 and 0.15.

(*ii*) *Fourier Self-Deconvolution of the Synthetic Spectra.* Fourier self-deconvolution of the synthetic spectra was carried out using a Lorentzian line shape, a FWHH of 14 cm^{-1}, and a resolution enhancement factor $(k)^3$ of 2.5. Using these parameters, we avoided the appearance of negative side lobes that are normally indicative of overdeconvolution. The number of bands detected was the same as in the derivative. The positions of the maxima in these deconvoluted spectra were in good agreement with the positions of the original bands.

(*iii*) *Curve-Fitting of the Synthetic Deconvoluted Spectra.* Fourier self-deconvolution and derivation gave the number and position of the component bands. The bandwidths and intensities were also estimated from the deconvoluted and derivated curves. These were the input parameters for a least-squares iterative curve-fitting (Fraser & Suzuki, 1966) that was performed to fit the bands with Gaussian line shape to the deconvoluted spectrum. The peak positions, heights, and bandwidths were allowed to vary simultaneously until a good fit was achieved. After comparing the curve-fitted bands with the original ones, we arrived at the following observations: (a) Taking each band individually, the respective integrated areas differed by 1–40% for the greater bands (more than 8% area). The two or three major bands usually showed errors less than about 7%, whereas some minor bands (less than 4% area) showed differences up to 90%. (b) Taking the curve-fitted bands in groups of two consecutive bands (neglecting the bands with an integrated intesity smaller than 2%), considering the sum of the two integrated areas, and comparing this value with the corresponding original summed areas, the errors were less than 15%. If groups of three consecutive bands were compared, the summed area errors were less than 10%.

(*iv*) *Experimental Spectra.* The method we followed with the experimental spectra of BR in H_2O and in D_2O suspension was as follows: (i) For IR spectra in H_2O, the signal to noise ratio in these spectra is greater than 400. We performed the third-order Fourier derivative using a breakpoint of 0.1. The parameters used for self-deconvolution were a FWHH of 14 cm^{-1} and a resolution enhancement factor of 2.5 [this value is less than log (S/N); see Mantsch et al. (1988)]. (ii) For IR spectra in D_2O, the signal to noise ratio is greater than 1000. The third-order derivative was performed using a breakpoint of 0.1 and a FWHH of 14 cm^{-1}, and k factors of 2.5 and 2.7 cm^{-1} were used for self-deconvolution. Due to the extensive band-crowding in the D_2O suspensions, the best experimental results were obtained by performing curve-fitting with the spectra deconvoluted with a k factor of 2.7. In both cases, curve-fitting over the deconvoluted spectra was done as described above for synthetic spectra.

RESULTS AND DISCUSSION

Assessment of Data. In deriving the secondary structure content of a protein by means of FTIR methods, it is important to first make an evaluation of the errors. We can distinguish two sources of errors in our procedure: (i) experimental errors, including possible differences among samples, detector non-linearity, uncompensated water vapor, and improper H_2O or D_2O subtraction; (ii) errors of the fitting process itself.

The experimental errors are shown in Table I as the standard deviations obtained from four independent samples. It can

[2] The wide-band MCT detector is linear to 3 AU, thus being highly suited for subtractions of water samples, which normally absorb to around 1 AU.

[3] The breakpoint used in Fourier derivation is the truncating point in the Fourier domain, which has the effect of smoothing the derivative. High breakpoint values allow high derivative efficiency, because more data points are used. The resolution enhancement factor (k) used in the deconvolution process is defined as the ratio between the bandwidth values before and after the mathematical treatment (Cameron & Moffatt, 1984).

Table I: Position, Fractional Areas, and Assignments of the Amide I Bands of Purple Membrane

H_2O			D_2O		
freq[a]	% area[b]	assignment	freq[a]	% area[b]	assignment
1689	3.1 ± 0.7	reverse turns	1690	2.0 ± 0.2	reverse turns
1680	7.3 ± 0.6	reverse turns	1683	4.9 ± 0.2	reverse turns
1673	5.4 ± 0.4	reverse turns	1674	6.5 ± 0.4	reverse turns
1665	22.1 ± 0.8	α_{II}	1666	21.9 ± 1.2	α_{II} + reverse turns
1658	23.0 ± 0.3	$\alpha_I + \alpha_{II}$	1658	15.5 ± 0.7	$\alpha_I + \alpha_{II}$
1650	11.2 ± 0.2	α + unordered	1652	12.9 ● 0.2	$\alpha + \alpha_I$
1642	9.9 ± 1.4	3_{10}-turns	1645	4.9 ± 0.4	unordered
1634	9.1 ± 0.7	β + C=N	1639	15.1 ± 2.0	3_{10}-turns + β
1627	3.4 ± 0.6	β	1633	2.8 ± 1.0	β
1619	4.7 ± 0.4	β	1626	7.4 ± 0.8	β + C=N
			1618	4.4 ± 0.3	β

[a] Frequency positions are expressed in cm^{-1} and are rounded off to the nearest integer. [b] Mean relative areas calculated from four independent experiments. The standard deviation is also indicated. The relative area values are also affected by the methodological error, as described in the text.

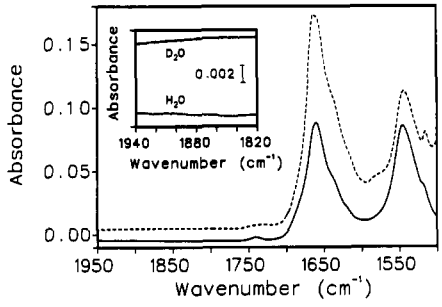

FIGURE 1: Absorption spectra of purple membrane suspensions in H_2O (—) and in D_2O (- - -), at an instrumental resolution of 1 cm^{-1}. Inset: The region above 1800 cm^{-1} expanded, to show the noise. The bar corresponds to 0.002 AU. Absorption spectra were obtained by coadding 1000 scans in blocks of 20 (20 sample scans and 20 reference scans) of the shuttle accessory, in order to minimize the water vapor bands.

be seen that the errors are low, at least for the most significant bands. The errors arising from the fitting procedure of the deconvoluted spectrum have been considered in detail under Materials and Methods. To summarize, pairs of consecutive bands will lead to errors less than 15%, whereas three or more consecutive bands reduce the errors to a maximum value of 10%. An additional source of error has been addressed: the influence of some amino acid side chain absorptions in the amide I region (Venyaminov & Kalnin, 1990). The exact contribution of these side chains is very difficult to quantify first because there are several unknown factors such as their ionization state or the nature of their environment and second because it is not known how these factors affect the amino acid side chain absorption. Thus, we simply estimated the amino acid contribution by using the values given by Venyaminov and Kalnin (1990), which correspond to aqueous amino acid models. The results showed that in the H_2O samples, the amino acid side chain contribution increased the original β-sheet content by about 2% and decreased the α-helix by another 2%. Thus, the side chain contribution can be considered negligible at this stage, but will be taken into account later.

Qualitative FTIR Results. The FTIR spectra of dark-adapted purple membrane suspensions in H_2O and D_2O are shown in Figure 1 for the amide I and II regions, with the ordinate values expanded in the 1820–1940-cm^{-1} region, to evaluate the presence of both random noise and residual water vapor bands.

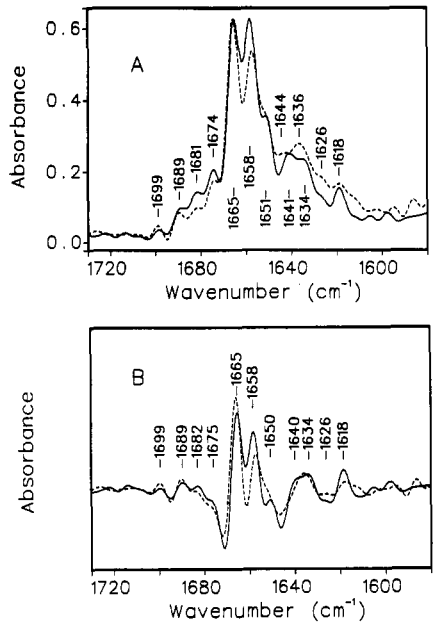

FIGURE 2: Resolution-enhanced amide I band of purple membrane suspensions in H_2O (—) and in D_2O (- - -). (A) Deconvoluted spectra, obtained using a bandwidth of 14 cm^{-1} and a k factor of 2.5. (B) Fourier-derivative spectra, obtained using a breakpoint of 0.1.

Figure 2 shows the deconvoluted and derivative spectra of BR in H_2O and D_2O. The two major maxima are at 1665–1666 and 1658 cm^{-1} in H_2O as well as in D_2O. These bands coincide almost exactly with the positions predicted by Krimm and Dwivedi (1982) for the α_{II}-helix (1667 and 1659 cm^{-1}) and α_I-helix (1659 and 1656 cm^{-1}), so that we assign these α-helical structures. Another possibility for the 1665–cm^{-1} band could be 3_{10}-helix (Kennedy et al., 1991). The band at 1650 cm^{-1} in H_2O should correspond to two different structures, α-helices and unordered structures, in accord with the well-accepted assignments for this region (Byler & Susi, 1986; Surewicz & Mantsch, 1988; Dong et al., 1990). In the D_2O spectrum, a band is present at about 1645 cm^{-1}; comparing both deconvoluted spectra, we can make the assumption that this band is the consequence of a shift from the 1650-cm^{-1} band and should correspond to unordered deuterated structure (Byler & Susi, 1986; Surewicz & Mantsch, 1988).

The assignment of the band at 1642 cm^{-1} in H_2O, which probably shifts to 1639 cm^{-1} in D_2O, is more difficult. These frequencies have been attributed normally to β-sheet structure. However, another likely possibility is 3_{10}-helix, as has been suggested for alamethicin (Haris & Chapman, 1988) and in a recent FTIR analysis of cytochrome b_5, on the basis of the X-ray structure (Holloway & Mantsch, 1989). If our secondary structure quantification has to agree with the latest structural determination (Henderson et al., 1990), this assignment is certainly more adequate. In fact, the 1642-cm^{-1} band can more properly correspond to isolated 3_{10}-turns, i.e., to type III β-turns. This would agree with theoretical calculations (Krimm & Bandekar, 1986) and with recent results concerning the assignment of type III β-turns to a band appearing at 1644–1646 cm^{-1}, using poly(α-aminoisobutyric acid) (Kennedy et al., 1991). Thus, the most likely interpretation of this band in accordance with the three-dimensional model is 3_{10}-helical turns. Otherwise, the calculated α-helical content would account for less than 50%.

The region between 1634 and 1619 cm^{-1} can be ascribed to different types of β-structure (Byler & Susi, 1986; Surewicz & Mantsch, 1988). Part of the β-structure corresponding to the 1634-cm^{-1} peak could shift after deuteration, and part

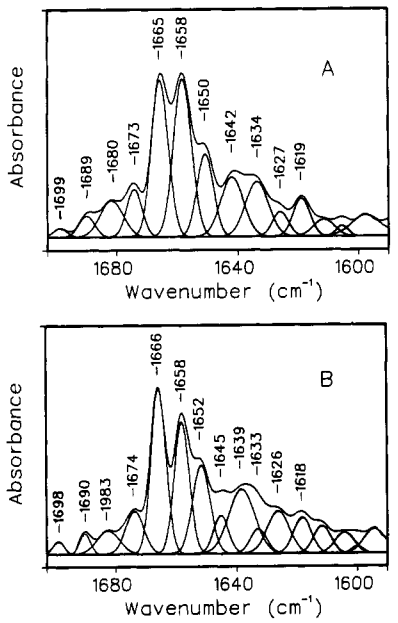

FIGURE 3: Deconvoluted spectra of purple membrane suspensions, with the best-fitted individual component bands. (A) In H_2O; (B) in D_2O. Deconvolution and band-fitting were done as indicated under Materials and Methods.

could rest overlapped with the 1639-cm^{-1} band. The 1619-cm^{-1} band in H_2O (1618 cm^{-1} in D_2O) could also arise from Tyr residues (Chirgadze et al., 1975). However, β-sheets have often been assigned to bands below 1620 cm^{-1} (Cabiaux et al., 1989; Fraser et al., 1991; Muga et al., 1990; Surewicz et al., 1990). Additionally, there is a band at about 1613 cm^{-1}, which can be due to Tyr residues. For these reasons, we assign preferentially this band to β-sheets. Finally, the four maxima at high wavenumbers (between 1670 and 1700 cm^{-1}) can be assigned mainly to reverse turns (Byler & Susi, 1986; Surewicz & Mantsch, 1988), although some weak contribution from β-structures is possible, and part of the 1699-cm^{-1} band could arise from carboxylic acids (Casal et al., 1988; Prestrelsky et al., 1991).

Quantitative FTIR Results. Curve-fitting procedures were carried out with four independent samples in order to consider the experimental errors. Figure 3 shows representative curve-fitting results for purple membrane samples suspended in H_2O and D_2O. Considering the maxima present in the derivative and deconvoluted curves, 14 bands (11 in the region 1619–1699 cm^{-1}) in H_2O and 15 bands (12 in the amide region) in D_2O were fitted to the deconvoluted spectra. The bands that do not correspond to the amide I were included to avoid the necessity of considering a base-line correction. Table I gives the mean relative areas with the respective standard deviation. The secondary structure assigned to each band is also indicated. At this point, we must understand these percentages in qualitative terms, because if the area of each band is considered individually the error could be high compared to the value of the original area (see the Materials and Methods).

In Table II, we consider groups of bands. In each group, the bands can be assigned normally to the same structural type or to similar types. As has been already indicated under Materials and Methods, when we consider groups of three or more bands after the curve-fitting is performed, the error of the summed area relative to that of the original bands is less than 10%. Then, in our curve-fitted spectra, we estimate the *maximum total error* by adding the methodological error (i.e., 10% error for three bands or 40% error for one band) to the experimental error (the standard deviation values of Table I).

Table II: Percent Composition of Secondary Structure of Purple Membrane[a]

H_2O			D_2O		
freq (cm^{-1})	area (%)	assignment	freq (cm^{-1})	area (%)	assignment
1689			1690		
1680	15.8 ± 2.6	turns	1683	13.4 ± 1.8	turns
1673			1674		
1665			1666		
1658			1658	50.3 ± 6.4	α
1650	66.2 ± 8.3	α + unordered	1652		
1642					
			1645	4.9 ● 2.4	unordered
1634					
1627	17.2 ± 2.7	β + C=N	1639	15.1 ± 8.0	$3_{10} + \beta$
1619					
			1633		
			1626	15.1 ● 2.8	β + C=N
			1618		

[a] The error shown corresponds to the sum of the experimental and the methodological errors (see Materials and Methods).

The bands between 1673 and 1690 cm^{-1} are assigned to reverse turns, so that in H_2O we obtain a total amount of turns of 15.8 ± 2.6%. In D_2O, the corresponding total amount is 13.4 ± 1.8%; the difference arises probably from a partial shift of some of these components to lower wavenumbers. We next consider the total α-helical content. Four bands in the H_2O spectra are assigned to α-helical structures: 1665, 1658, 1650, and 1642 cm^{-1}, but the band at 1650 cm^{-1} has two components (α-helix plus unordered structure). From the curve-fitted bands in H_2O, we cannot determine directly the amount of unordered structure. However, in D_2O, the band at 1645 cm^{-1} can be assigned to this type of structure, and adding the methodological error (40%) to the experimental one, we obtain a value of 4.9 ± 2.4% for unordered structure. The area of the α-helical bands in H_2O is 66.2 ± 8.3%. Assuming that the H → D exchange has been almost complete for unordered structure, we can obtain the total α-helical content by subtraction, giving a final value of 61.3 ± 10.7% (in H_2O). On the other hand, the quantification of the helical structures from the D_2O samples gives a similar result as that obtained from the H_2O samples, provided that some reverse turn absorptions shift to a position under the α-helical bands and that some β-sheet components appear under the 1639-cm^{-1} band.

The mean area in the region of β-sheet structures (between 1634 and 1618 cm^{-1}) is 17.2 ± 2.7% in H_2O, and 15.1 ± 2.8% in D_2O. This difference must be due to the presence of some β-component that has remained at 1639 cm^{-1} in D_2O (in H_2O, this weak band is not detected individually). However, two considerations argue that these percentages should be decreased. First, a Schiff base stretching vibration band should be present in this region (Earnest et al., 1990), that we cannot detect directly. This band should appear at 1636 cm^{-1} in H_2O and at 1626 cm^{-1} in D_2O. An increment of about 4% is observed in the band at 1626 cm^{-1} after deuteration; however, this value is uncertain due to the high error involved. Second, the subtration of the amino acid side chain contribution should have the effect of slightly decreasing the absorption of the 1600–1640-cm^{-1} region. These two effects cannot be quantified properly, but we could set a lower amount of about 4% (at least 2% for each effect). Thus, our final estimation for the mean β-sheet content is about 13%.

Comparison of our deconvoluted spectra with those published previously by other authors reveals the presence of more

constituent bands in our spectra. As an example, Lee et al. (1987) reported FTIR spectra at 4 cm^{-1} which, after deconvolution in the amide I region, showed bands at 1685, 1675 (shoulder), 1661, 1637, and 1619 cm^{-1} for the purple membrane suspended in 1 M KCl/10 mM HEPES, pH 6.8. Later, Earnest et al. (1990) presented polarized FTIR spectra at 2-cm^{-1} resolution with peaks at 1685, 1676, 1665, 1656/1658, 1639, 1631, and 1618 cm^{-1} for hydrated purple membrane films. It seems clear that some of the bands in these spectra are splitted into two or more components in our spectra. In this sense, the 1685-cm^{-1} peak described by Earnest et al. (1990) is split into the bands at 1690 and 1680 cm^{-1}, the peak at 1639 cm^{-1} gives rise to the 1642- and 1636-cm^{-1} bands, and the 1631-cm^{-1} one to the 1633- and 1627-cm^{-1} bands. Additionally, the 1650-cm^{-1} band was not detected by these authors.

Structural Implications. The overall quantification of the secondary structure of native bacteriorhodopsin can be summarized as being 52–73% α-helices, 13–19% reverse turns, 11–16% β-sheets, and 3–7% unordered segments. The α-helices appear to be distributed mainly in two different classes, corresponding to α_I and α_{II} (about 45% in total). We propose the existence of type III β-turns (amounting 10–13%), thus having characteristics similar to isolated 3_{10}-helical turns. Also, another slightly different α_I-helical class (about 5%) appears at 1650 cm^{-1} in H_2O. It should be noted that this splitting of the α_I absorption into two different bands does not necessarily indicate that presence of different helical classes. For example, one helical side could contribute to one IR band, whereas the other side, possessing a slightly different environment, could contribute to another IR band (Goormaghtigh et al., 1990). From Table I, we can infer that there is a majority of α_{II}-helices (about 22% plus an undetermined amount coming from the 1658-cm^{-1} band). This agrees with the estimations of Gibson and Cassim (1989) from CD studies. In accordance with previous findings (Downer et al., 1986; Earnest et al., 1990; Englander & Englander, 1977), only about 25% of the total structures exchange protons with deuterons. It appears that the α^{II} segments do not exchange at all. This suggests that these segments are forming the most inner part of the membrane-spanning α-helices. On the other hand, part of α_I appears to exchange with deuterons, whereas the putative 3_{10}-turns seem to exchange completely. Thus, it may be hypothesized that these last helices are located in the most accessible or most external parts of the transmembrane rods. A possible location for the 3_{10}-helices could be the last turn of the transmembrane helices, similar to what is observed for the globular proteins (Richardson, 1981). This gives about 28 amino acids presumably involved in this class of helices, or about 11%, which is similar to the experimentally obtained value.

Taking into account all sources of errors and the uncertainties in the band assignments, it seems safe to conclude that a substantial amount of reverse turns exist in BR (at least 13%). This is in accordance with the predictions of White and Jacobs (1990), who described a high probability of finding reverse turns in all the links, with the higher probability corresponding to the C-terminal segment. Also, Vogel and Gärtner (1987) reported Raman studies on bacterioopsin which yielded values of 11–17% reverse turns. Thus, if we suppose that each link has a reverse turn, plus one reverse turn located on the C-terminal segment (i.e., a total of seven reverse turns), this gives an estimate of 11% reverse turns, a figure very similar to what we deduce from our spectra. In addition, it is conceivable that some links could pertain to the category of nonregular secondary structure termed *omega loops* defined for the globular proteins, which frequently contain reverse turns (Leszczynski & Rose, 1986). In this case, it is probable that the small percentage of unordered structure arises mainly from the amino acids forming the loops (excluding those involved in the reverse turns), plus some from the C-terminal tail.

The relatively high proportion of β-sheets that is calculated from our spectra requires some comments. Actually, there are several reasons to think that this value should be decreased somewhat. First, the contributions of both the amino acids and the Schiff base C=N stretching band have been set to a minimum, because we have no means to obtain the exact value; second, the 1619/1618-cm^{-1} band could arise partially from Tyr residues. It should be noted that a diminished β-sheet content would be more in accord with Raman (Vogel & Gartner, 1987) and CD (Nabedryk et al., 1985) results. Nevertheless, even a lower content such as a possible consensus value around 10% presents the problem of the location of these structures. Henderson et al. (1990) suggested that the short cytoplasmatic links are forming extended polypeptide chains. However, if we accept a content of at least 11% reverse turns and the above distribution (one reverse turn per loop), then there are not enough amino acids on the links of the cytoplasmatic side to form any significant amount of extended structures. In fact, the links and the two terminal tails are the most uncertain parts of the electron diffraction map. In this sense, the dense features seen in the N-terminal side could probably also be interpretated as containing some extended chains. This would be more in agreement with the lesser amount of α-helices calculated by us (52–73%) compared with a total of 72–76% derived from the work of Henderson et al. (1990) for the sum of the transmembrane helices (66%), plus some 6–10% arising from the noncytoplasmatic links.

ACKNOWLEDGMENT

We thank M. Duñach, J. Manyosa, and D. Garcia-Quintana for critical reading of the manuscript and R. Henderson for sending us the BR coordinates.

REFERENCES

Braiman, M. S., Mogi, T., Marti, T., Stern, L. J., Khorana, H. G., & Rothschild, K. J. (1988) *Biochemistry 27*, 8516–8520.
Byler, D. M., & Susi, H. (1986) *Biopolymers 25*, 469–487.
Cabiaux, V., Brasseur, R., Wattiez, R., Falmagne, P., Ruysschaert, J.-M., & Goormaghtigh, E. (1989) *J. Biol. Chem. 264*, 4928–4938.
Cameron, D. G., & Moffatt, D. J. (1984) *J. Test. Eval. 12*, 78–85.
Casal, H. L., Köhler, U., & Mantsch, H. H. (1988) *Biochim. Biophys. Acta 957*, 11–20.
Chirgadze, Y. N., Fedorov, O. V., & Trushina, N. P. (1975) *Biopolymers 14*, 679–694.
Dencher, N. A. (1983) *Photochem. Photobiol. 38*, 753–767.
Dong, A., Huang, P., & Caughey, W. S. (1990) *Biochemistry 29*, 3303–3308.
Dousseau, F., & Pézolet, M. (1990) *Biochemistry 29*, 8771–8779.
Downer, N. W., Bruchman, T. J., & Hazzard, J. H. (1986) *J. Biol. Chem. 261*, 3640–3647.
Duñach, M., Padrós, E., Muga, A., & Arrondo, J. L. R. (1989) *Biochemistry 28*, 8940–8945.
Earnest, T. N., Herzfeld, J., & Rothschild, K. J. (1990) *Biophys. J. 58*, 1539–1546.
Englander, J. J., & Englander, S. W. (1977) *Nature 265*, 658–659.

Fodor, S. P. A., Ames, J. B., Gebhard, R., van der Berg, E. M. M., Stoeckenius, W., Lugtenburg, J., & Mathies, R. A. (1988) *Biochemistry 27*, 7097–7101.
Fraser, E. D. B., & Suzuki, E. (1966) *Anal. Chem. 38*, 1770–1773.
Fraser, P. E., Nguyen, J. T., Surewicz, W. K., & Kirschner, D. A. (1991) *Biophys. J. 60*, 1190–1201.
Gibson, N. J., & Cassim, J. Y. (1989) *Biochemistry 28*, 2134–2139.
Glaeser, R. M., Downing, K. H., & Jap, B. K. (1991) *Biophys. J. 59*, 934–938.
Goormaghtigh, E., Cabiaux, V., & Ruysschaert, J.-M. (1990) *Eur. J. Biochem. 193*, 409–420.
Haris, P. I., & Chapman, D. (1988) *Biochim. Biophys. Acta 943*, 375–380.
Henderson, R., Baldwin, J. M., Ceska, T. A., Zemlin, F., Beckmann, E., & Downing, K. H. (1990) *J. Mol. Biol. 213*, 899–929.
Holloway, P. W., & Mantsch, H. H. (1989) *Biochemistry 28*, 931–935.
Kennedy, D. F., Crisma, M., Toniolo, C., & Chapman, D. (1991) *Biochemistry 30*, 6541–6548.
Khorana, H. G. (1988) *J. Biol. Chem. 263*, 7539–7442.
Krimm, S., & Dwivedi, A. M. (1982) *Science 216*, 407–408.
Krimm, S., & Bandekar, J. (1986) *Adv. Protein Chem. 38*, 181–364.
Lee, D. C., Herzyk, E., & Chapman, D. (1987) *Biochemistry 26*, 6775–5783.
Lee, D. C., Haris, P. I., Chapman, D., & Mitchell, R. C. (1990) *Biochemistry 29*, 9185–9193.
Lee, D. C., Haris, P. I., Chapman, D., & Mitchell, R. C. (1991) in *Spectroscopy of Biological Molecules* (Hester, R. E., & Girling, R. B., Eds.) pp 7–10, Royal Society of Chemistry, Herts, U.K.
Leszczynski, J. F., & Rose, G. D. (1986) *Science 234*, 849–855.
Lin, G. C., El-Sayed, M. A., Marti, T., Stern, L. J., Mogi, T., & Khorana, H. G. (1991) *Biophys. J. 60*, 172–178.
Mantsch, H. H., Moffatt, D. J., & Casal, H. (1988) *J. Mol. Struct. 173*, 285–298.
Moffatt, D. J., Kauppinen, J. K., Cameron, D. G., Mantsch, H. H., & Jones, R. N. (1986) *Computer programs for infrared spectrophotometry*, NRCC Bulletin 18, National Research Council of Canada, Ottawa, Canada.
Muga, A., Surewicz, W. K., Wong, P. T. T., Mantsch, H. H., Singh, V. K., & Shinohara, T. (1990) *Biochemistry 29*, 2925–2930.
Nabedryk, E., Bardin, A. M., & Breton, J. (1985) *Biophys. J. 48*, 873–876.
Oesterhelt, D., & Stoeckenius, W. (1974) *Methods Enzymol. 31*, 667–678.
Oesterhelt, D., & Tittor, J. (1989) *Trends Biochem. Sci. 14*, 57–61.
Prestrelsky, S. J., Arakawa, T., Kennedy, W. C., & Byler, D. M. (1991) *Arch. Biochem. Biophys. 285*, 111–115.
Richardson, J. S. (1981) *Adv. Protein Chem. 34*, 167–339.
Stoeckenius, W., & Bogomolni, R. (1982) *Annu. Rev. Biochem. 52*, 587–616.
Surewicz, W. K., & Mantsch, H. H. (1988) *Biochim. Biophys. Acta 952*, 115–130.
Surewicz, W. K., Leddy, J. J., & Mantsch, H. H. (1990) *Biochemistry 29*, 8106–8111.
Venyaminov, S. Yu., & Kalnin, N. N. (1990) *Biopolymers 30*, 1243–1257.
Vogel, H., & Gärtner, W. (1987) *J. Biol. Chem. 262*, 11464–11469.
White, S. H., & Jacobs, R. E. (1990) *J. Membr. Biol. 115*, 145–158.